SAND2016-7735C

Severe Accident Modeling for Cyber Scenarios

Jeff Cardoni, Matt Denman, Tim Wheeler

Sandia National Laboratories: P.O. Box 5800, Albuquerque, NM, 87185-0748, jncardo@sandia.gov

INTRODUCTION

A generic severe accident model of a PWR is developed to support analyses of cyber-fault scenarios that may lead to extensive core damage. For this purpose, a MELCOR 2.1 [1] model of a generic PWR is created that is capable of simulating primary and secondary thermal-hydraulics, core heatup and fuel degradation, RPV failure, containment response, and radionuclide release and transport to the environment. The size and detail of the severe accident model are intended to facilitate scoping analyses of various cyber-based scenarios in an automated, dynamic framework. A dynamic job scheduler such as ADAPT [2] will be used to evaluate many accident scenarios in an automated fashion utilizing parallel computing. Individual test calculations are first conducted of a basic unmitigated scenario (i.e. no significant operator intervention) with a cyber-based accident initiator. This preliminary assessment is used to gauge modelling capabilities for further, expanded cyber accident scenarios in conjunction with ADAPT.

SEVERE ACCIDENT MODEL

The MELCOR code (version 2.1) is used in this work to evaluate severe accident progression and source terms for a generic PWR. MELCOR is a severe accident and source term code developed by Sandia National Laboratories (SNL) for the Nuclear Regulatory Commission (NRC).

A reasonably detailed and robust MELCOR model of a PWR with sub-atmospheric containment is developed. This efforts calls for a fast and stable model that is capable of simulating many variations and sensitivity/uncertainty studies of the chosen base accident sequences. Thus, the model must be simple enough to permit fast execution and minimize errors, but it must also contain sufficient resolution to provide mechanistic evaluation of severe accidents.

Nodalization Summary

MELCOR inputs for the dynamic simple cyber (DSC) model have been completed for the core, RPV, RCS, containment, auxiliary building, and safeguards building. This includes decay heat and inventory inputs, as well as control functions that support the operation of valves and pumps.

Table I provides a summary of the size and complexity of the current DSC model. It compares the number of MELCOR elements that are most important for run-time and user-interaction/friendliness. The number of control volumes and flow paths (especially in the core region) are most important for CPU time considerations. The number of COR cells, lower head nodes, and heat structures are usually of second order importance for CPU time and code performance, and thus these features have not been reduced as much compared to large plant models. Also, sufficient heat structure resolution is required for reasonable predictions of radionuclide deposition.

Table I. RCS and containment nodalization summary.

MELCOR element	#
COR cells	86
RPV lower head nodes	60
Control volumes	36
Flow paths	58
Heat structures	90

The nodalization of the core, RPV, primary and secondary RCS, and containment are described further in the following subsections. Most of the heat structures are not depicted in the nodalization diagrams. However, the DSC model contains an appropriate level of heat structure modeling fidelity to support predictions of radionuclide transport and deposition. Several heat structures are used to represent the vessel steel, core barrel, RCS piping, pressurizer steel, and steam generator components (e.g. steam generator tubes). All heat structures between the RCS and containment are assumed to be covered by insulation. Several volumes also contain internal heat structures such as the control rod guide tubes and housings in the upper regions of the RPV.

Core and RPV

Fig. 1 shows the 2-D MELCOR representation of the core and lower plenum in the DSC model. This is the COR package nodalization of the MELCOR model, and it only represents the spatial domain for solid materials. The spatial domain for fluid flow is coarser to facilitate calculation stability and reduce CPU time requirements. Structural heat transfer, stresses, and material relocation are resolved on the spatial nodalization depicted in Fig. 1, and these calculations receive thermal-hydraulic feedback from the fluids packages in MELCOR.

The purple material in Fig. 1 denotes fuel bundles (fuel and cladding) and the yellow material is structural support,

which is mostly stainless steel. The active core is discretized into 50 nodes (five rings and ten axial levels). Seven levels are used to represent the lower plenum, five of which are for the multi-level core support plate. Like the core region, most of the lower plenum is also comprised of five rings, excluding a 6th ring that only exists at the second axial level to represent the region below the downcomer. In total, the core and lower plenum are nodalized by 86 COR cells. The use of several core nodes and a multi-level core plate allows for an estimation of gradual core degradation, which is physically and computationally more desirable than a model that degrades/relocates the entire core instantaneously.

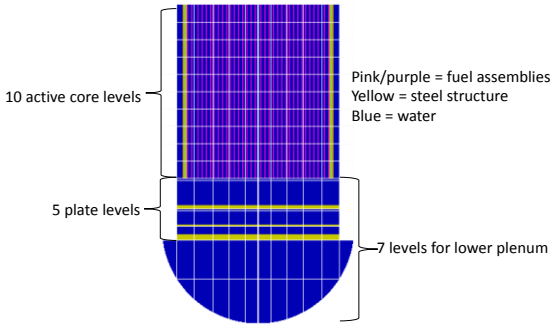

Fig. 1. Core nodalization in DSC model.

Only gross failure of the lower head is considered in the DSC model. Penetration failure or other unique RPV failure modes are not considered. MELCOR determines lower head failure using 1-D stress calculations and 2-D heat transfer over a coarse mesh that represents the lower head. The lower head mesh in the DSC is comprised of 60 total nodes that correspond to six azimuthal segments and ten through-wall nodes. Gross lower head failure only occurs after severe core damage and material relocation following support failure. The DSC model treats core debris in the lower plenum as a porous debris bed and it neglects debris coolability limitations (the 0D Lipinski coolability model is not invoked), which are both MELCOR best-practices.

Fig. 2 shows the control volumes (black blocks) and flows paths (blue and red arrows) used to represent the RPV. Fig. 2 illustrates an axisymmetric view of the RPV, and it lists some of the main elevations in the model that are relative to the bottom of the RPV. The blue arrows are nominal flow paths that are always 'open,' while the red arrows depict flow paths that 'open/close' dynamically based on MELCOR predictions. For example, flow may develop between the channel and bypass volumes if MELCOR predicts the core shroud/baffle structure (treated in the COR package) to fail.

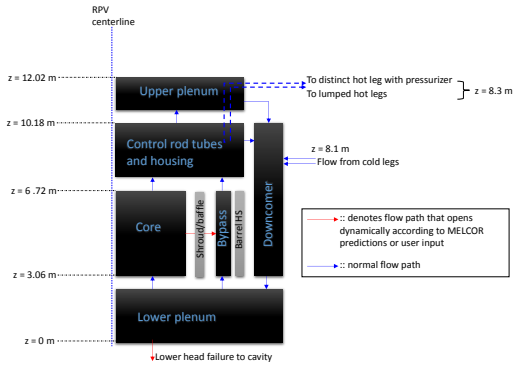

Fig. 2. RPV hydrodynamic nodalization in DSC model.

RCS

The RCS nodalization for the DSC model represents a multi-loop PWR; the number of loops is currently arbitrary. The coolant loop with the pressurizer is treated distinctly in order to better assess pressurizer valve cycling and potential creep ruptures. The remaining loops are lumped together to decrease the number of volumes, flow paths, and heat structures. Counter-current natural circulation, which occurs once the hot leg is mostly steam and hot gases, is approximated using MELCOR's internal submodel via the FL_CCF input record.

Fig. 3 depicts the nodalization of the primary RCS. Each coolant loop is separated into four volumes (2 hot leg volumes, 2 cold leg volumes), and the surge line and pressurizer each have one volume. Currently, the pressurizer has one PORV and one SRV that discharge flow to the surge tank. The rupture disk flows to the relief tank cubicle in the containment; it is assumed to open once the relief tank pressure reaches 100 psig. Dynamic flow paths are implemented for potential creep rupture for each hot leg and the surge line.

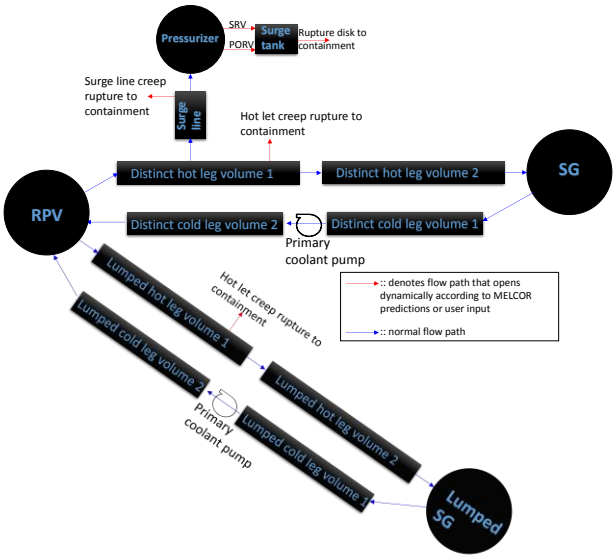

Fig. 3. Primary RCS nodalization.

Fig. 4 shows the nodalization of the steam generators. The black volumes in Fig. 4 denote primary-side SG regions, and the orange volumes denote the secondary side. The primary side of the SGs is nodalized into two volumes–one for upward flow through the SG tubes and one for downward flow. These volumes are thermally linked to secondary side SG-boiler volume via heat structures that represent the SG tubes. Saturated steam produced in the boiler region flows to the SG dome volume and then to the steam line volume, which is connected to a time-independent turbine volume via the MSIV flow path. Currently, each steam line has one SRV that connects the steam lines to the environment, which is also a time-independent volume. Main feedwater and TDAFW are represented by mass sources into the SG boiler volumes. Dynamic flow paths for SGTR may open based on MELCOR predictions (i.e. simple creep rupture) or due to sequence boundary conditions.

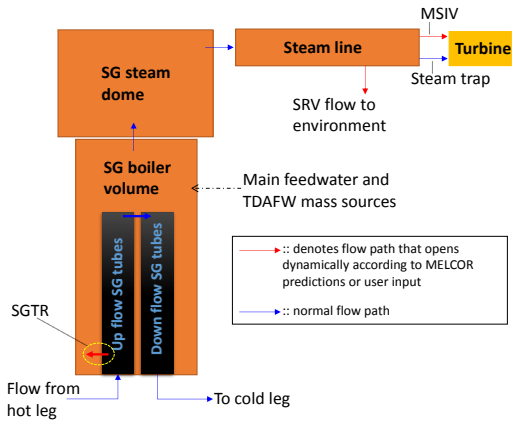

Fig. 4. Steam generator nodalization.

Containment and Buildings

The containment in the DSC model is based on previous SNL PWR severe accident research [3]. It contains 8 control volumes, 17 internal flow paths, and 34 heat structures for proper accounting of radionuclide deposition and thermal inertia in the containment. The DSC model uses one MELCOR CAV component to simulate molten core-concrete interactions (MCCI) in the cavity after RPV lower head failure.

The auxiliary and safeguards buildings are represented simply with one control volume each, along with pertinent heat structures for radionuclide deposition. Both buildings have flow paths to the environment. Containment bypass leakage through the LHSI piping leads to the safeguards building, while RHR leakage flows to the auxiliary building. Additional leak paths to the environment that are represented in the model include containment design leakage, enhanced containment leakage due to overpressure (based on [3]), and the SRVs off the steam lines.

TEST RESULTS

A containment bypass leak via the RHR piping is a credible cyber-fault accident scenario. Therefore, a scoping calculation of an SBO in conjunction with RHR leakage is conducted with the DSC model. For the purposes of this test calculation, it is assumed that the RHR system is located in the auxiliary building and its piping penetrates the containment in order to received water from the hot legs and inject water into the cold legs.

Loss of offsite power is defined to start at t=0, after which the reactor trips, feedwater into SGs ceases, and the primary pumps coast down. Three hours after initiation of the accident, check valves for the RHR system are assumed to open simultaneously allowing ingress of primary coolant from the hot leg. Much of the RHR piping is not rated for primary-side pressures, and hence it is assumed that the piping ruptures outside the containment soon (5 minutes) after the check valves open; this allows the primary RCS to blow down though the RHR piping and to the auxiliary building, creating a containment bypass flow path for radionuclides and accelerating coolant loss from the RCS.

Fig. 5 depicts the RPV pressure response for the SBO with RHR leakage. The initial three hours of the accident resembles a basic SBO scenario: decay heat is removed from the primary RCS via the steam generators until the secondary water inventory is exhausted. Afterwards, the primary RCS heats up and pressurizes to the pressurizer SRV setpoint, which discharges coolant inventory to the pressurizer relief tank and ultimately to the containment; Fig. 6 shows the resulting containment pressure. After three hours, the RHR check valves open and the pressure in the RHR piping immediately increases to the primary pressure (near 16 MPa); the RHR piping outside containment then ruptures 5 minutes later. The primary RCS blows down to the auxiliary building, as evident by the rapid RPV depressurization shortly after 3 hours in Fig. 5. In contrast to a typical SBO, depressurization of the primary RCS does not pressurize the containment since the coolant bypasses the containment to the auxiliary building via the RHR piping.

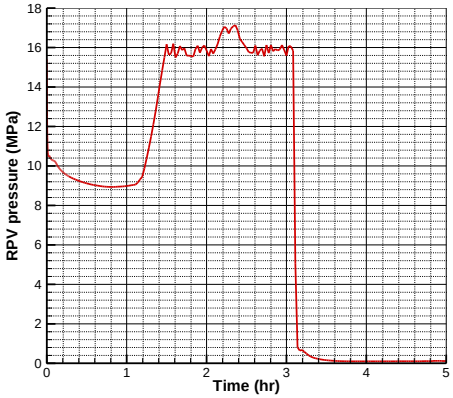

Fig. 5. RPV pressure.

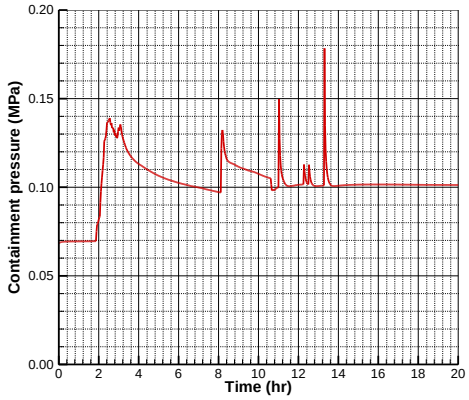

Fig. 6. Containment pressure.

Fig. 7 show the water level, relative to the bottom of the RPV, for the SBO with RHR leakage. In this figure, the top of active fuel is near 6.72 m and the bottom of active fuel is near 3.06 m. In-vessel oxidation of Zircaloy cladding and core steel structures begins around 2.8 hours when the core water level is near BAF. MELCOR predicts about 290 kg of hydrogen gas to be generated by in-vessel oxidation reactions, as shown by Fig. 8.

Fig. 9 depicts the radionuclide deposition in the RHR piping, with values normalized to the respective initial core inventories of each class. MELCOR predicts significant long-term deposition of radionuclides in the RHR piping for the more volatile main group (Cd), alkali metal group (Cs), the less volatile main group (Sn), and the early transition elements (Mo). Other classes deposit in significant amounts but later re-vaporize and move to the auxiliary building, such as the halogens (I) and chalcogens (Te).

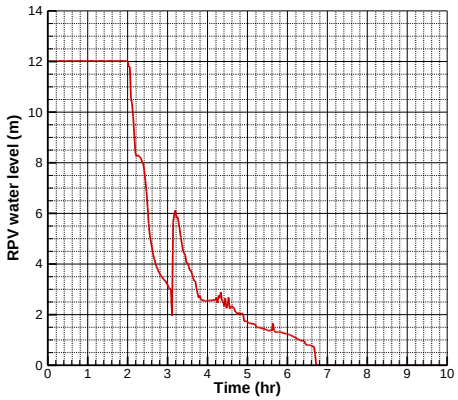

Fig. 7. RPV water level.

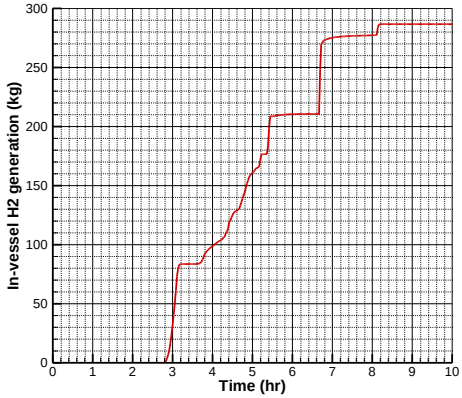

Fig. 8. In-vessel hydrogen generation.

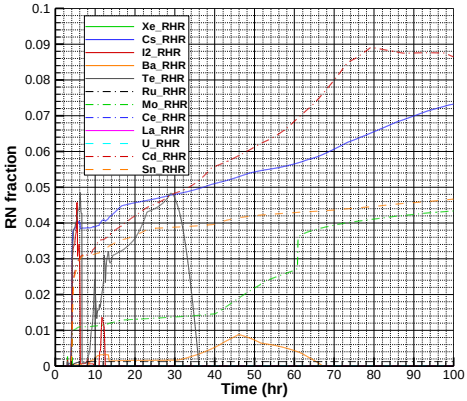

Fig. 9. Radionuclide deposition in RHR piping.

SUMMARY AND FUTURE WORK

A MELCOR model of a generic PWR with sub-atmospheric containment has been developed for simulations of cyber-fault severe accidents. The model has the capability to simulate the cyber-related accident initiator and the subsequent severe accident progression, including radionuclide source terms. Future analyses will investigate additional cyber-related scenarios in an automated and dynamic framework using ADAPT.

REFERENCES

1. L.L. Humphries, et al., "MELCOR Computer Code Manuals, Vol. 2: Reference Manuals, Version 2.1.6840," SAND2015-6692R, Sandia National Laboratories, Albuquerque, NM (2015).
2. D. Kunsman, et al., "Development and Application of the Dynamic System Doctor to Nuclear Reactor Probabilistic Risk Assessments," SAND2008-4746, Sandia National Laboratories, Albuquerque, NM (2008).
4. US. NRC, "State-of-the-Art Reactor Consequence Analysis Project, Volume 2: Surry Integrated Analysis," NUREG/CR-7110, Volume 2, U.S. Nuclear Regulatory Commission: Washington D.C. (2012).